The Stochastic Piston Problem

G. Lin, C.-H. Su and G.E. Karniadakis *
Division of Applied Mathematics
182 George Street
Brown University
Providence, RI 02912
Classification: Physical Sciences: Applied Mathematics

August 9, 2004

Abstract

We obtain analytical solutions for the perturbed shock paths induced by time-varying random motions of a piston moving inside an adiabatic tube of constant area. The variance of the shock location grows *quadratically* with time for early times and switches to *linear* growth for longer times. The analytical results are confirmed by stochastic numerical simulations, and deviations for large random piston motions are established.

The English physicist James Joule was perhaps the first to use the concept of a *moving piston* in order to demonstrate the mechanical equivalent of heat in his pioneering studies, almost two centuries ago. The moving piston has also been used extensively in fundamental studies of fluid mechanics and shock discontinuities in the last century, and this now classical problem has been solved analytically in one- and also higher space dimensions (1, 2). It is well known that a shock wave propagating into a stationary fluid sets it into motion and raises its pressure, temperature and density. This situation can be physically realized by a planar, cylindrical or spherical piston moving at specified speed into a stagnant fluid. In gasdynamics, in particular, in the context of normal shock waves, the one-dimensional classical problem describes a piston moving at *constant* speed in a tube of constant area and adiabatic walls; the shock wave is created ahead of the piston. Solutions of this flow problem with arbitrary piston speeds are difficult to obtain even for the one-dimensional case, although recently approximate analytical solutions have been obtained for accelerating and decelerating pistons valid only for short times, e.g. see (3).

In the current work we revisit the one-dimensional piston problem within the stochastic framework, i.e., we allow for random piston motions which may be changing in time. In particular, we superimpose small random velocity fluctuations to the piston velocity and aim to obtain analytical solutions of the stochastic flow response. Within the context of small random fluctuations, we assume that the same thermodynamic conditions are valid as in the classical problem, i.e., that an isentropic region exists between the piston surface and the shock wave. This assumption is justified by the theory of weak shocks although at the microscopic level more complex processes may take place. For example, it has been reported in (4) that a wall, which is adiabatic when rigidly fixed, may become conducting when it is allowed to have a stochastic motion independently of the value of its macroscopic velocity.

*Corresponding author, Email: gk@dam.brown.edu; Tel: 401-863-1217; Fax: 4018-63-2722

Report Documentation Page

Form Approved
OMB No. 0704-0188

1. REPORT DATE	2. REPORT TYPE	3. DATES COVERED
09 AUG 2004		**00-08-2004 to 00-08-2004**

4. TITLE AND SUBTITLE	5a. CONTRACT NUMBER
The Stochastic Piston Problem	5b. GRANT NUMBER
	5c. PROGRAM ELEMENT NUMBER
6. AUTHOR(S)	5d. PROJECT NUMBER
	5e. TASK NUMBER
	5f. WORK UNIT NUMBER
7. PERFORMING ORGANIZATION NAME(S) AND ADDRESS(ES) **Brown University,Division of Applied Mathematics,182 George Street,Providence,RI,02912**	8. PERFORMING ORGANIZATION REPORT NUMBER
9. SPONSORING/MONITORING AGENCY NAME(S) AND ADDRESS(ES)	10. SPONSOR/MONITOR'S ACRONYM(S)
	11. SPONSOR/MONITOR'S REPORT NUMBER(S)

12. DISTRIBUTION/AVAILABILITY STATEMENT
Approved for public release; distribution unlimited

13. SUPPLEMENTARY NOTES

14. ABSTRACT

15. SUBJECT TERMS

16. SECURITY CLASSIFICATION OF:			17. LIMITATION OF ABSTRACT	18. NUMBER OF PAGES	19a. NAME OF RESPONSIBLE PERSON
a. REPORT **unclassified**	b. ABSTRACT **unclassified**	c. THIS PAGE **unclassified**		**10**	

However, in the macroscopic models we develop here we will assume that such effects are negligible and thus all surfaces remain adiabatic.

In the first part of the paper, we employ stochastic perturbation analysis to obtain closed-form analytical formulas for the perturbed shock paths. The random piston motion is modeled as a stochastic process following a Markov chain corresponding to various values of correlation length. The main physical finding extracted from the analytical solution is that the variance of the location of the perturbed shock grows quadratically with time at early times but it switches to linear growth at later times. In the second part of the paper, we perform high-resolution stochastic simulations using a standard Monte Carlo approach and also using the polynomial chaos method based on Wiener-Hermite expansions. The objective is to confirm the results of perturbation analysis and determine their validity range using numerical solutions of the full nonlinear Euler equations subject to stochastic inputs. More generally, the stochastic piston problem we have defined here serves as a strict testbed for rigorous evaluation of numerical stochastic solvers, and to this end, we have compared the performance of polynomial chaos against the Monte Carlo approach. The results depend critically on the specific value of correlation length as well as on the length of time integration. At early times and/or large values of correlation length the polynomial chaos method outperforms (often by orders of magnitude) the Monte Carlo approach, however it is not as effective in other cases.

1 Stochastic Perturbation Analysis

We consider a piston having a constant velocity, U_p, moving into a straight tube filled with a homogeneous gas at rest. A shock wave will be generated ahead of the piston. A sketch of the piston-driven shock tube with random piston motion superimposed is shown in Fig. 1. Given the state ahead of the shock, the speed of the shock, S, and the thermodynamic states of the gas behind the shock (i.e., ahead of the piston) are determined in terms of the piston speed through the conservation of mass, momentum and energy (5). For perfect gas with constant specific heats, these relations are:

$$\frac{\rho_0}{\rho_1} = 1 - \frac{U_p}{S} \tag{1a}$$

$$\frac{P_1}{P_0} = 1 + \frac{\gamma}{c_0^2} S U_p \tag{1b}$$

$$S = \frac{\gamma+1}{4} U_p + \sqrt{\left(\frac{\gamma+1}{4} U_p\right)^2 + C_0^2} \tag{1c}$$

where $\gamma = c_p/c_v$ is the ratio of specific heats, and C_0 is the local sound speed ahead of the shock. The sound speed behind the shock can be obtained from Eqs. 1a and 1b:

$$C^2 = (C_0^2 + \gamma S U_p)(1 - U_p/S). \tag{2}$$

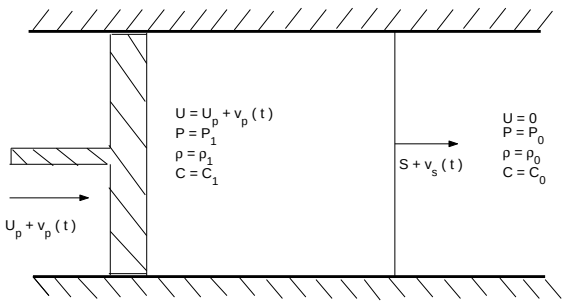

Figure 1: Sketch of piston-driven shock tube with random piston motion.

In the following we will normalize all velocities with C_0, and thus $C_0 = 1$. We now define the stochastic motion of the piston by superimposing a small stochastic component to the steady speed of the piston, i.e.,

$$u_p(t) = U_p[1 + \epsilon V(t, \omega)], \tag{3}$$

where the amplitude ϵ is small, $0 < \epsilon \ll 1$. Our objective is to find how do the perturbed shock paths due to the random piston motion deviate from the unperturbed ones; the latter are given by

$$X(t) = S \cdot t. \tag{4}$$

Under the small amplitude assumption, the flow field induced by this perturbation can be obtained based on the assumption that the propagation speed in the region behind the shock and ahead of the piston can be identified as the propagation speed of the unperturbed flow quantities, i.e., $U_p \pm C$, where C is the unperturbed sound speed behind the steadily moving shock as given by Eq. 2.

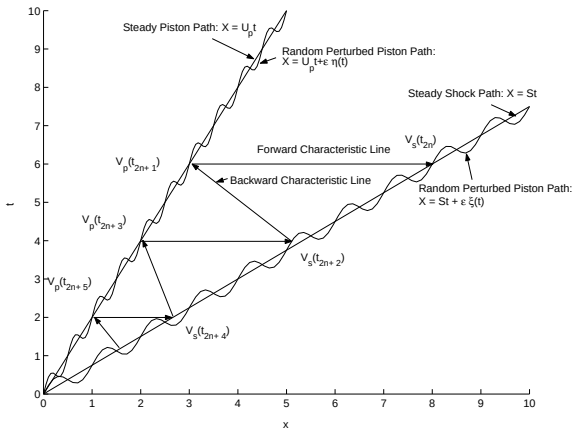

Figure 2: A sketch of shock paths induced by random piston motions.

To proceed we consider the perturbed Riemann's invariants and evaluate them at the shock from

$$(1 \pm k) v_s = j_\pm = v_p \pm \frac{2}{\gamma - 1} a_p, \quad \text{with} \quad k = C \frac{S + S' U_p}{1 + \gamma S U_p}, \tag{5}$$

where $S' = \frac{dS}{dU_p}$, and v_p, a_p and $j_\pm$ are, correspondingly, the perturbed piston velocity, the perturbed local sound speed, and the perturbed Riemann's invariants. These invariants are constant along the *unperturbed* (straight) characteristic lines. For more details on this derivation and on the assumptions, the interested reader is referred to (6). Fig. 2 shows a sketch of the shock paths induced by random piston motions. Specifically, the distorted lines show an instantaneous realization of the piston path and shock path. They are distorted due to induced reflections as sketched in the plot via the characteristic lines. In the sketch, the steady and perturbed piston paths are denoted by $U_p t$ and $U_p t + \epsilon\ \eta(t)$ while those for the shock paths by $S\, t$ and $S\, t + \epsilon\ \xi(t)$. Also, $v_p(t_{2n+1})$ and $v_s(t_{2n})$ are on the *forward* characteristic $\frac{dx}{dt} = U_p + C$; $v_s(t_{2n+2})$ while $v_p(t_{2n+1})$ is on the *backward* characteristic $\frac{dx}{dt} = U_p - C$. Thus, we have through the use of the Riemann invariants in Eq. (5), that:

$$(1 + k) v_s(t_{2n}) = v_p(t_{2n+1}) + \frac{2}{\gamma - 1} a_p(t_{2n+1}) \tag{6a}$$

$$(1 - k) v_s(t_{2n+2}) = v_p(t_{2n+1}) - \frac{2}{\gamma - 1} a_p(t_{2n+1}). \tag{6b}$$

Adding Eqs. 6a and 6b to eliminate $a_p(t_{2n+1})$, we obtain the following recurrence formula:

$$v_s(t_{2n}) = q v_p(t_{2n+1}) - r v_s(t_{2n+2}), \quad n = 0, \ldots, N, \ldots \tag{7}$$

where

$$q = \frac{2}{1 + k} \ \text{ and } \ r = \frac{1 - k}{1 + k}.$$

Eq. 7 defines a recursive relationship between the velocities at the shock and the perturbation of the piston motion $v_p(t)$. Starting at time t_0 and iterating up to N, we obtain from Eq. 7 a set of $(N+1)$ terms. Eliminating $v_s(t_2)$, $v_s(t_4) \ldots v_s(t_{2N})$ from this set we obtain

$$v_s(t) = q \sum_{n=0}^{N} (-r)^n v_p(t_{2n+1}) + (-r)^{N+1} v_s(t_{2N+2}). \tag{8}$$

If the perturbation of the piston starts at time $t_s > 0$, the zigzag path of the characteristics coming down to the origin will end on the piston path; therefore, v_s in the last term in Eq. 8 is zero. On the other hand, if $t_s = 0$, the zigzag path will zigzag indefinitely to approach $t = 0$ i.e., $N \to \infty$. Since r is always less then unity, the last term of Eq. 8 will approach zero for any finite value of $v_s(t_\infty)$. Therefore, one can drop the last term in Eq. 8 to obtain:

$$v_s(t) = q \sum_{n=0}^{N} (-r)^n v_p(t_{2n+1}), \tag{9}$$

where $N = \infty$ if $t_s = 0$, i.e., the perturbation of the piston starts at $t = 0$ or it is determined by the last non-zero value of $v_p(t_{2N+1})$.

To make effective use of this relation we need to obtain the relationship of the shock locations at t_{2n}, t_{2n+1} and t_{2n+2}. To this end, let us denote the shock locations at time t_{2n} and t_{2n+2} by $X_s(t_{2n})$ and $X_s(t_{2n+2})$, correspondingly, and the piston location at t_{2n+1} by $X_p(t_{2n+1})$. Assuming the characteristics are approximated by straight lines with their slopes given by $U_p \pm C$, we have

$$\begin{aligned} X_s(t_{2n}) - X_p(t_{2n+1}) &= (U_p + C)(t_{2n} - t_{2n+1}) \\ X_p(t_{2n+1}) - X_s(t_{2n+2}) &= (U_p - C) \\ &\quad (t_{2n+1} - t_{2n+2}). \end{aligned} \tag{10}$$

Also, defining the perturbed path of the shock and the piston by $\xi(t)$ and $\eta(t)$, we can express

$$\begin{aligned} X_s(t_{2n}) &= S \cdot t_{2n} + \epsilon\xi(t_{2n}), \\ X_s(t_{2n+2}) &= S \cdot t_{2n+2} + \epsilon\xi(t_{2n+2}), \\ X_p(t_{2n+1}) &= U_p t_{2n+1} + \epsilon\eta(t_{2n+1}). \end{aligned}$$

Finally, substituting these into Eq. 10, we obtain

$$\begin{aligned} t_{2n+1} = \alpha t_{2n} + \frac{\epsilon}{C}[\eta(t_{2n+1}) &- \xi(t_{2n})] \\ t_{2n+2} = \beta t_{2n} + \epsilon\gamma[2\eta(t_{2n+1}) &- \xi(t_{2n}) \\ &- \xi(t_{2n+2})], \end{aligned} \tag{11}$$

where

$$\begin{aligned} \alpha &= \frac{C + U_p - S}{C} < 1 \\ \beta &= \frac{C + U_p - S}{C + S - U_p} < 1 \\ \gamma &= \frac{1}{C + S - U_p} < 1. \end{aligned}$$

The inequalities above are due to $C > 1$ and $S > U_p$.

If we drop the term containing ϵ in Eq. 11, which is consistent with the small disturbance assumption, the recurrent relationship is very much simplified and closed form solutions can be obtained. (We will retain this term in the next subsection below). With this simplification we have that:

$$\begin{aligned} t_{2n+1} = \alpha t_{2n} = \alpha\beta t_{2n-2} = \alpha\beta^2 t_{2n-1} \ldots &= \alpha\beta^n t_0 \\ &= \alpha\beta^n t. \end{aligned}$$

Eq. 8 then reads as

$$v_s(t) = q\sum_{n=0}^{N}(-r)^n v_p(\alpha\beta^n t), \tag{12}$$

and the shock speed is then obtained as

$$S(U_p + v_s(t)) = S(U_p) + \frac{dS}{dU_p}v_s(t) = S + S'v_s(t),$$

with the shock path governed by

$$\frac{dX_s}{dt} = S + S'v_s(t).$$

Using Eq. 11 we have

$$\epsilon\frac{d\xi}{dt} = qS'\sum_{n=0}^{\infty}(-r)^n v_p(\alpha\beta^n t), \tag{13}$$

and taking $\xi(0) = 0$, we obtain

$$\xi(t) = \frac{qS'}{\epsilon}\sum_{n=0}^{\infty}(-r)^n \int_0^t dt_1 v_p(\alpha\beta^n t_1). \tag{14}$$

As a check of Eq. 12, we first consider the simple problem of a piston with its velocity subject to a small *constant* perturbation v_p starting at $t = 0$ (e.g., a step function of size v_p). According to Eq. 13, we have

$$v_s(t) = q\sum_{n=0}^{\infty}(-r)^n v_p(t_{2n+1}) = qv_p\sum_{n=0}^{\infty} -r^n = v_p$$

i.e., the velocity behind the shock will be $U_p + v_p$ for all $t > 0$. The shock speed S will change to $S(U_p + v_p)$, instead of $S(U_p)$.

We now consider v_p to be a random process with zero mean and the following covariance

$$v_p(t) = \epsilon U_p V(t, \omega) \tag{15a}$$

$$\left.\begin{aligned} &\langle V(t,\omega)\rangle = 0 \\ &\langle V(t_1,\omega), V(t_2,\omega)\rangle = e^{-\frac{|t_1 - t_2|}{A}} \end{aligned}\right\} \tag{15b}$$

where A is the correlation time. The above covariance kernel describes a Markov random process in time. The larger the value of the correlation time A is the closer the random motion approaches a fully-correlated process - we refer to this as a *random variable* case. On the other hand, the smaller the value of the correlation time A is the closer the motion resembles white noise.

Substituting Eq. 15a into 14, we obtain

$$\xi(t) = qS'U_p \sum_{n=0}^{N} (-r)^n \int_0^t dt_1 V(\alpha\beta^n t_1, \omega).$$

Because of Eq. 15b, we have

$$\begin{aligned} \langle \xi(t) \rangle &= 0 \\ \langle \xi^2(t) \rangle &= (U_p q S')^2 \sum_{n=0}^{\infty}\sum_{m=0}^{\infty} (-r)^{m+n} \\ &\quad \int_0^t dt_1 \int_0^t dt_2 e^{-\frac{\alpha}{A}|\beta^n t_1 - \beta^m t_2|}. \quad (16) \end{aligned}$$

The double summation in Eq. 16 can be split into three parts: 1. sum of all diagonal terms, 2. sum of all the terms above the diagonal, and 3. the terms described in detail below. It is easy to see, that the last two sums are equal. Thus, we have

$$\begin{aligned} \langle \xi^2(t) \rangle &= (U_p q S')^2 \left[2 \sum_{n=1}^{\infty}\sum_{m=0}^{n-1} (-r)^{n+m} \int_0^t dt_1 \right. \\ &\quad \int_0^t dt_2 e^{-\frac{\alpha}{A}|\beta^n t_1 - \beta^m t_2|} \\ &+ \left. \sum_{n=0}^{\infty} (r^{2n}) \int_0^t dt_1 \int_0^t dt_2 e^{-\frac{\alpha\beta^n}{A}|t_1 - t_2|} \right]. \end{aligned}$$

Both integrals in the above equation can be integrated explicitly to give

$$\langle \xi^2(\tau) \rangle = (U_p q S' A/\alpha)^2 \left[2 \sum_{n=1}^{\infty}\sum_{m=0}^{n-1} (-r)^{n+m} I_{n,m}(\tau) + \sum_{n=0}^{\infty} r^{2n} I_{n,n}(\tau) \right] \quad (17)$$

where $\tau = \alpha t/A$, and

$$I_{n,m}(\tau) = \frac{2\tau}{\beta^m} + \frac{1}{\beta^{n+m}} \left[e^{-\beta^m \tau} + e^{-\beta^n \tau} - 1 - e^{-(\beta^m - \beta^n)\tau} \right],$$

where $m < n$. For $\tau \ll 1$ it is easy to show that $I_{n,m} = \tau^2$. The summations in Eq. 17 can be performed explicitly to obtain

$$\langle \xi^2(\tau) \rangle \approx (U_p q S' A/\alpha)^2 \frac{\tau^2}{(1+r)^2} \text{ for } \tau \ll 1. \quad (18)$$

For $\tau \gg 1$, we can neglect the exponential terms in equation (1), and thus

$$I_{n,m}(\tau) = \begin{cases} \dfrac{2\tau}{\beta^m} - \dfrac{1}{\beta^{n+m}} & \text{for } m < n \\ \dfrac{2\tau}{\beta^n} - \dfrac{2}{\beta^{2n}} & \text{for } m = n \end{cases}$$

These expressions for $I_{n,m}$ can again be summed analytically on the right-hand-side of Eq. 17, to obtain

$$\langle \xi^2(\tau) \rangle \approx (U_p q S' A/\alpha)^2 \left[\frac{2\tau(1-r)}{(1-r^2/\beta)(1+r)} - \frac{2}{(1-r^2/\beta^2)(1+r/\beta)} \right], \text{ for } \tau \gg 1 \quad (19)$$

For arbitrary values of τ, we calculate the quantities in the square brackets in Eq. 17 numerically. Because of the smallness of the values of r and β, the series converges fast. We plot in Fig. 3 the quantity $\langle \xi^2(\tau) \rangle / (U_p q S' A/\alpha)^2$ as a function of τ given by Eq. 17 with $U_p = 1.25$ i.e., corresponding to Mach number of the shock $M = 2$. The asymptotic formula for small and large τ given in Eqs. 18 and 19 are also included in the plot. We observe a *qualitative* change in the stochastic response versus time. At early times, the location of the path scales linearly with time whereas at later times it scales with square root of time (note that the variance $< \xi >^2 \sim (Length)^2$). This interesting result is consistent with physical intuition suggesting that at early times convective motions dominate while at longer times the diffusion process takes over.

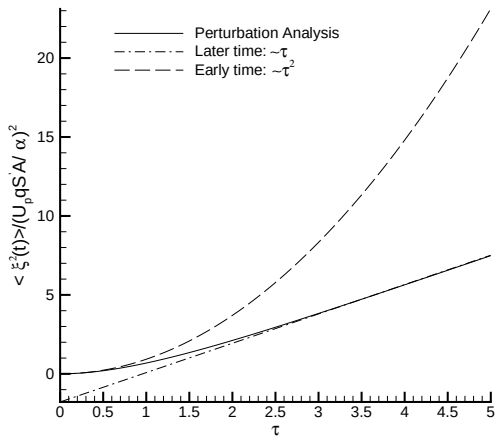

Figure 3: Normalized variance of perturbed shock paths. Solid line: perturbation analysis results, see equation (17); Dashed line: early-time asymptotic results from Eq. 18; Dash-Dotted line: late-time asymptotic results from Eq. 19.

Within the context of small amplitude random motions of the piston, we have neglected the last term in Eq. 11 involving ϵ. This allowed us to obtain closed-form analytical solutions, as we explained in the previous section. Now we revisit this approximation and retain that term, so we employ the following recurrence formulas:

$$\begin{aligned} t_{2n+1} &= \alpha t_{2n} + \frac{\epsilon}{C}[\eta(t_{2n+1}) - \xi(t_{2n})] \\ t_{2n+2} &= \beta t_{2n} + \epsilon\gamma[2\eta(t_{2n+1}) - \xi(t_{2n}) - \xi(t_{2n+2})] \end{aligned}$$

where α, β and γ are given in Eq. (12). For a general n, we have the following sequence:

$$\begin{aligned} t_{2n} &= \beta t_{2(n-1)} + \epsilon\gamma[2\eta(t_{2n-1}) - \xi(t_{2(n-1)}) \\ &\quad -\xi(t_{2n})] \\ t_{2(n-1)} &= \beta t_{2(n-2)} + \epsilon\gamma[2\eta(t_{2n-3}) - \xi(t_{2(n-2)}) \\ &\quad -\xi(t_{2(n-1)})] \\ t_{2(n-2)} &= \beta t_{2(n-3)} + \epsilon\gamma[2\eta(t_{2n-5}) - \xi(t_{2(n-3)}) \\ &\quad -\xi(t_{2(n-2)})] \\ &\cdots\cdots \\ t_2 &= \beta t + \epsilon\gamma[2\eta(t_1) - \xi(t) - \xi(t_2)]. \end{aligned} \tag{20}$$

Solving for t_{2n} from the above equations, we obtain:

$$\begin{aligned} t_{2n} =& \beta^n t + \epsilon\gamma[\sum_{j=1}^{n} 2\eta(t_{2j-1})\beta^{n-j} - (1+\beta) \\ & \sum_{j=1}^{n-1} \xi(t_{2j})\beta^{n-j-1} - \xi(t_{2n}) - \beta^{n-1}\xi(t)] \end{aligned} \tag{21}$$

Thus, t_{2n+1} can be expressed as:

$$\begin{aligned} t_{2n+1} = \beta^n[\alpha t - \frac{\epsilon\xi(t)}{C}] + \frac{\epsilon}{C}[2\beta\sum_{j=1}^{n}\eta(t_{2j-1})\beta^{n-j} + \\ \eta(t_{2n+1})] - \frac{\epsilon(1+\beta)}{C}\sum_{j=1}^{n}\beta^{n-j}\xi(t_{2j}) \end{aligned} \tag{22}$$

The shock path is governed by

$$\epsilon\frac{d\xi}{dt} = qS'\sum_{n=0}^{\infty}(-r)^n v_p(t_{2n+1}),$$

and taking $\xi(0) = 0$, we have

$$\xi(t) = \frac{qS'}{\epsilon}\sum_{n=0}^{\infty}(-r)^n\int_0^t dt_1 v_p(t_{2n+1}). \tag{23}$$

Considering Eqs. 15b and 23 together, we obtain

$$\begin{aligned} \langle\xi(t)\rangle &= 0 \\ \langle\xi^2(t)\rangle &= (U_p qS')^2\sum_{n=0}^{\infty}\sum_{m=0}^{\infty}(-r)^{m+n}\int_0^t dt_1 \\ &\quad \int_0^t dt_2 e^{-\frac{1}{A}|t_{1,2n+1} - t_{2,2m+1}|} \end{aligned} \tag{24}$$

To compute the variance of the induced shock path $\langle \xi^2(t) \rangle$ we need to compute t_{2n+1}. However, Eq. 22 shows that to compute t_{2n+1} we have to know the shock path $\xi(t)$ at all the previous reflection times t_{2j+1} and t_{2j}. To this end, we solve Eqs. 21 22, 23 and 24 numerically, by employing an iteration method and setting $t_{2j+1} = \alpha\beta^j t$ and $t_{2j} = \beta^j t$ as an initial approximation.

In the following section, we perform stochastic numerical simulations to confirm our findings and establish limitations of the stochastic perturbation analysis presented in this section.

2 Stochastic Simulations

We perform two types of stochastic simulations to verify the results of the previous section, following a Monte Carlo approach and a polynomial chaos approach. We employ the full nonlinear Euler equations with the extra complication that there is an unsteady stochastic boundary, namely the piston position. To this end, a boundary-fitted coordinate approach is employed to transform the equations into a stationary domain. The transformed Euler equations contain stochastic source terms proportional to $-\rho\partial u_p/\partial t$ and $-\rho v\partial u_p/\partial t$ in the momentum and energy equations, respectively.

In Monte Carlo simulations, we use a Markov chain in time to represent the *stochastic input*. In polynomial chaos simulations, the representation of *stochastic inputs* is expressed by a Karhunen-Loeve decomposition; see references (7, 8). Specifically, we consider different representations of the stochastic inputs corresponding to the covariance kernel

$$< V(t_1,\omega)V(t_2,\omega) >= e^{\frac{-|t_1-t_2|}{A}}, \qquad (25)$$

where A is the correlation length. A corresponding Markov chain is employed to represent discretely the exponential kernel as follows:

$$\begin{aligned} V_0 &= \xi_0 \\ V_1 &= CV_0 + f\xi_1 \\ &\cdots\cdots \\ V_{i+1} &= CV_i + f\xi_{i+1} \end{aligned}$$

where

$$C = e^{\frac{-\Delta t}{A}} \quad \text{and} \quad f = \sqrt{1-C^2}.$$

In the Monte Carlo simulation, a random piston velocity $u_p = U_p(1+\epsilon V_i(t,\omega))$ is selected from the above Markov chain as a stochastic input at each time step t_i. In the polynomial chaos representation we employ Wiener-Hermite expansions for all conservative and derived stochastic variables of the form

$$X(\omega) = \sum_{j=0}^{M} \hat{x}_j \Phi_j(\boldsymbol{\xi}(\boldsymbol{\omega})), \qquad (26)$$

where the basis $\{\Phi_j\}$ is formed from the Hermite orthogonal polynomials of degree p. Here $\xi(\omega)$ is a Gaussian variable of dimension N and M is the total number of deterministic coefficients $\hat{x}_j$, where $M+1 = (N+p)!/(N!p!)$. We employ the fifth-order WENO method in space in order to capture the shock location accurately and the third-order TVD Runge-Kutta method in time; see details in (9).

We now present some results for the following conditions: Behind the shock we impose a steady piston velocity: $U_p = 1.25$ (normalized by the sound speed ahead of the shock), i.e., corresponding to Mach number of the shock $M = 2$. Ahead of the shock the sound speed is $C_o = 1$ and the pressure is $P = 1$. We investigate the stochastic response for various values of the correlation length A and of the amplitute of the random piston motion ϵ.

In Fig. 4, we plot the variance of the perturbed shock paths induced by small random piston motions corresponding to amplitude $\epsilon = 0.01$ and correlation lengths $A = 0.5, 1, 2$ and 10 obtained from Monte Carlo simulations (2,000 runs). There is good agreement of the Monte Carlo solutions with the analytical

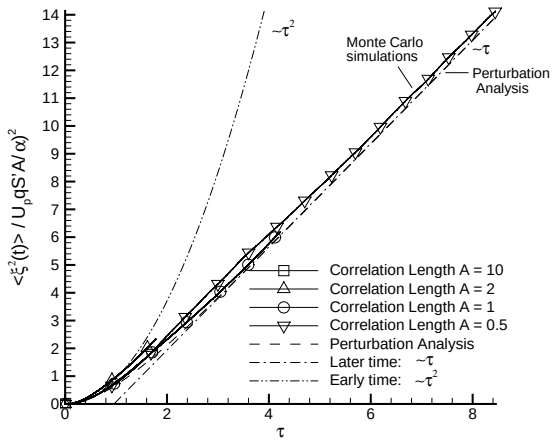

Figure 4: Solid line: Variance of the perturbed shock paths for $\epsilon = 0.01$ and $A = 0.5, 1, 2$ and 10 obtained from Monte Carlo simulations; Dashed line: results from perturbation analysis; Dash-Dotted line: results from equation (19) for later time; Dash-Dot-Dotted line: results from equation (18) for early time.

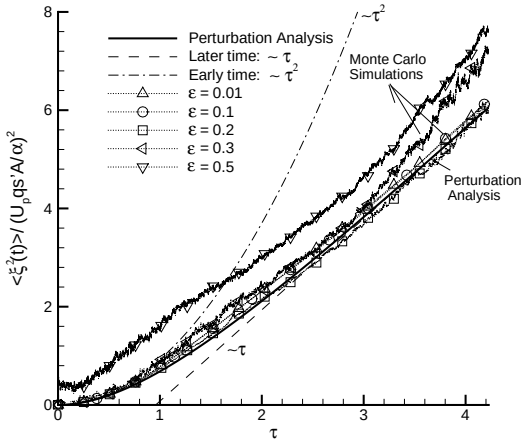

Figure 5: Dotted line: Variance of the perturbed shock paths for $A = 1$ and $\epsilon = 0.01, 0.1, 0.2, 0.3$ and 0.5 obtained from Monte Carlo simulations; Solid line: results from perturbation analysis; Dashed line: results from equation (19) for later time; Dash-Dotted line: results from equation (18) for early time.

solutions. In Fig. 5, we plot the variance of the perturbed shock paths induced by random piston motions corresponding to correlation length $A = 1$ and amplitudes $\epsilon = 0.01, 0.1, 0.2, 0.3$ and 0.5 obtained from Monte Carlo simulations (3,000 runs). For small amplitudes $\epsilon = 0.01, 0.1$ and 0.2, good agreement is observed between Monte Carlo simulations and analytical solution. However, for larger amplitude, such as $\epsilon = 0.3$ and 0.5, the stochastic simulation deviates from the analytical solution. We will examine this discrepancy in some more detail below but first we present results from the polynomial chaos simulations.

Fig. 6 shows results from polynomial chaos simulations corresponding to piston motions described by a *random variable*, i.e. a fully-correlated stochastic process whereby $A \to \infty$. The polynomial chaos simulations match quite closely the exact analytical solutions even over a more than *two-orders of magnitude change* in the value of the variance. This verifies the convergence of Hermite-chaos for this case. Fig. 7 shows results from polynomial chaos simulations corresponding to piston motions described by a *random process* with amplitude $\epsilon = 0.01$ and correlation time $A = 1$. In the polynomial chaos simulations, the number of stochastic dimensions of random input is changed from $N = 3, 6, 50$ to 100 (N is also the number of Karhunen-Loeve modes for representing the stochastic piston motion). By increasing the dimensions of random input, the polynomial chaos simulations agree better with the analytical solution longer. However, there is a finite error after long time integration unlike the Monte Carlo simulations.

We now re-examine what is the effect of neglecting the second term in Eq. (11), which we included in the refined perturbation analysis of the previous section. In Fig. 8, we compare the variance of the perturbed shock paths with large $U_p + v_p(t)$ random piston mo-

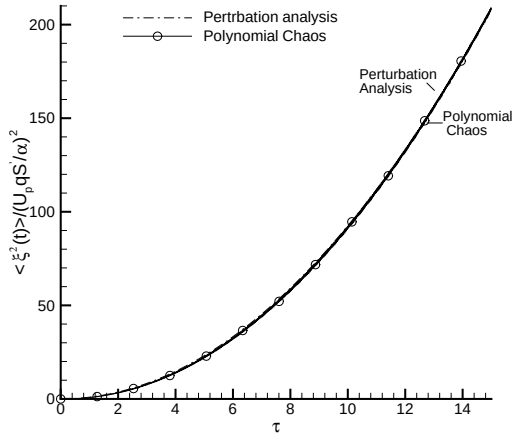

Figure 6: Variance of the perturbed shock paths for a *random variable* (fully-correlated kernel, $A \to \infty$) with amplitude $\epsilon = 0.01$. Dash-Dotted line: analytical solution from perturbation analysis; Solid line: numerical results from polynomial chaos simulations.

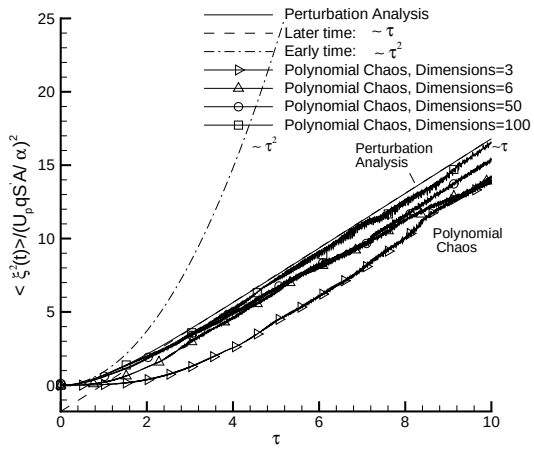

Figure 7: Variance of the perturbed shock paths for $\epsilon = 0.01$ and $A = 1$ obtained from polynomial chaos simulations with stochastic dimensions $N = 3, 6, 50$ and 100.

tions obtained from Monte Carlo simulations, analytical solutions from perturbation analysis, and analytical results obtained including the corrections for larger random piston motions. Indeed, significant improvement in the semi-analytical results is evident compared to Monte Carlo simulations.

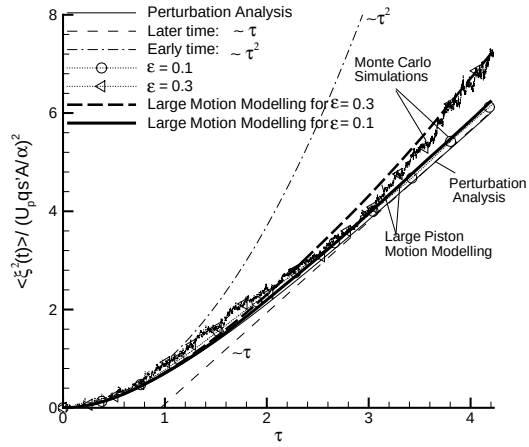

Figure 8: Thick-Solid line and Thick-Dashed line: Variance of the perturbed shock shock paths corresponding to correlation length $A = 1$, amplitudes $\epsilon = 0.1$ and 0.3 obtained from larger random piston motion modeling; Dotted line: results from Monte Carlo simulations; Solid line: results from perturbation analysis; Dashed line: results from equation (19) for later time; Dash-Dotted line: results from equation (18) for early time.

3 Summary

The stochastic piston problem is a re-formulation, within the stochastic framework, of a classical aerodynamics problem that studies how small random piston motions affect shock paths. We have developed an analytical solution for the linearized Euler equations for the *stochastic* piston problem. Specifically, Eqs. (17),

(18) and (19) represent the main analytical results of this paper. The first equation gives the full analytical expression whereas the last two give asymptotic results for early times and longer times, respectively. They reveal that the variance of the location of the perturbed shock paths grows initially quadratically with time and switches to linear dependence for longer times. The stochastic numerical simulations presented in the paper confirm the results and show good agreement with the analytical solution for up to 20% amplitudes of the random piston motion compared to the mean steady motion.

Acknowledgements

This work was supported by the Computational Mathematics program of AFOSR and DOE. Computations were performed at Brown's TCASCV, University of Illinois/NCSA and University of California/NPACI facilities.

References

1. Courant, R. & Friedrichs, K.O.. *Supersonic Flows and Shock Waves*. Interscience Publishers, Inc., 1948.

2. Whitham, G.B.. *Linear and Nonlinear Waves*. John Wiley & Sons, Inc., 1974.

3. Lazarev, M.P., Prasad, P. & Singh, S.K.. An approximate solution of one-dimensional piston problem. *ZAMP*, 46:752–771, 1995.

4. Gruber, c. & Frachebourg, L.. On the adiabatic properties of a stochastic wall: Evolution, stationary non-equilibrium, and equilibrium states. *EPFL, Lausanne, preprint*, 2004.

5. Liepmann, H.W. & Roshko, A.. *Elements of Gas Dynamics*. John Wiley & Sones, Inc., 1957.

6. Su, C.-H.. Shock paths induced by small random piston motions: A perturbation analysis. *Report, Center for Fluid Mechanics, Brown University*, 2004.

7. Ghanem, R.G. & Spanos, P.. *Stochastic Finite Eelements: A Spectral Approach*. Springer-Verlag, New York, 1991.

8. Xiu, D. & Karniadakis, G.E.. The Wiener-Askey polynomial chaos for stochastic differential equations. *SIAM J. Sci. Comput.*, 24(2):619–644, 2002.

9. Jiang, G.-S. & Shu, C.-W.. Efficient implementation of weighted ENO schemes. *J. of Comput. Phys.*, 126:202–228, 1996.